ARTICLE

In situ sediment biodegradation via a sediment microbial fuel cell and steel-slag: I. Electricity generation

Received 00th January 20xx,
Accepted 00th January 20xx

DOI: 10.1039/x0xx00000x

Kyeongmin Kim [a], Shinya Nakashita *[a] and Tadashi Hibino [a]

Steel-slag was added as a catalytic material of redox potential to sediment microbial fuel cells (SMFCs) in an situ sediment biodegradation experiment to determine the benefits on the long-term power production of the cells and to elucidate the external factors affecting power production. The steel-slag was found to consistently increase the power generated, and over a period of two years, the combination produced six times more charge than that of an SMFC alone (1,549 C/day), which was superior to that of conventional SMFCs reported in the literature. Upon investigation, rapid changes or fluctuations in power production were found to be cathode-related, for example, if it was damaged or variations in the ambient environmental conditions, such as the dissolved oxygen, algal activity, etc., affected its performance. In particular, algal activity appeared within nine days, which led to a 68% increase in the average current density during the day vs. the night. In summary, the addition of steel-slag improved the power production of the SMFC over a two-year period and the most important external factor was found to be algal activity on the cathode. To address this, there is a need to monitor the inevitable biofilm growth that occurs in in situ.

Introduction

The Fukuyama inner bay is located in the Seto Inland Sea, Japan (34°28'52"N, 133°22'55"E), which is a semi-enclosed shelf sea connected to the Pacific Ocean. A map of this area is shown in Fig. 1. Wastewater has been discharged in this coastal region from nearby industry complexes at various times in the past (about 60 times per year during rainfall),[1] and even though the volume of wastewater discharged has been reduced to 40% of past levels, blue tides are still observed throughout the year, which suggests that significant contamination loads and oxygen depletion remain. Moreover, as the topography of this area is narrow and long (i.e., a maximum width of approximately 500 m and a total length of approximately 8 km), the water exchange rate is very low, which allows high concentrations of contaminants to accumulate in the seabed. Consequently, water contamination in this urban coastal region has become a severe challenge and the removal of contaminants in these sediments is an increasingly important part of mitigating growing risks to the environment to prevent the continued release of water contaminants over the long term.[2]

Microbial fuel cells (MFCs) have attracted interest as a potential candidate for future alternative energy production. Moreover, researchers have recently begun to shift their interest towards bioremediation beyond energy production.[3] Sediment microbial fuel cells (SMFCs), which are a type of MFC, have an anode embedded in the anoxic sediments and a cathode suspended in the aerobic water column. This configuration is promising for both bioremediation of contaminated sediment and electricity generation.[4,5] One application of SMFC technology that has been studied over several years is the biodegradation of organic compounds,[6–9] and it has been found in indoor experiments that SMFCs can support biodegradation in organic carbon, such as total organic carbon, total petroleum hydrocarbons, polycyclic aromatic hydrocarbons, etc. Nevertheless, the potential of SMFCs for in situ biodegradation of contaminated sediment remains largely unexplored, which is likely due to the higher complexity of open water bodies and the associated study and control processes.[10] From a practical point of view, it is worth noting that the natural redox potential difference between oxic water and anoxic sediments is generally below 0.8 V.[11] When the inevitable overpotential of SMFCs are taken into consideration, the actual electrode potential may be insufficient or inappropriate to drive the transformation needed to reduce the level of contamination.[12] We have so far been demonstrated a steel-slag via indoor experiments as a way to overcome this limitation as its addition reduces the anode potential to around -646 mV (vs. Ag/AgCl) via a redox reaction with Fe. The steel-slag has been shown to ensure a sufficient difference in the potentials to increase the current of the SMFC.

In this study, an in situ experiment was conducted using an SMFC and steel-slag over a two-year period at the Fukuyama inner bay. The main objective was to demonstrate the potential increase in power production of an SMFC with steel-slag in the field. In addition, the influence of various external factors occurring in the actual environment are evaluated on the SMFC system in detail (e.g., the tide, dissolved oxygen, algal activity, maintenance, etc.). It is anticipated that the results of this study will provide useful insights into the practical operation of SMFCs in actual conditions with respect to both power production and remediation of a benthic environment. It should be noted that the specific focus of this paper is on the catalytic role of steel-slag in anode performance from a long-term perspective while

[a] Graduate School of Engineering, Hiroshima University, Kagamiyama 1-4-1, Higashi-Hiroshima, Hiroshima, 739-8527, Japan.

Electronic Supplementary Information (ESI) available: [details of any supplementary information available should be included here]. See DOI: 10.1039/x0xx00000x

the details of conventional SMFCs in situ have been discussed in a separate paper.[13]

Materials and methods

Preparation of SMFC and steel-slag

The SMFC was prepared as per the detailed description provided in a previous study[14] and carbon fiber (E-C-CC1-06, Electro-Chem) was employed as an electrode. The carbon fiber (0.18 m^2) was pre-treated by heating at 500 ℃ for 30 min to increase its performance as an electrode as per Nagatsu et al[15] and the anode and cathode were connected by Ti and Cu wires to an external resistance of 1.4 Ω under closed-circuit conditions. The voltage between the anode and cathode across the external load was measured using a voltage recorder (VR-71, T&D Corp.) and the cathode electrode potential was periodically measured with respect to an Ag/AgCl electrode placed near the cathode. The recorded voltage was converted into current using Ohm's law (*current = voltage / resistance*) and the electric charge quantity was determined using the equation *electric charge = current × time*. The power was calculated as per *power = current × voltage* and the current and power densities were normalized by dividing these values by the surface area of the anode.

The steel-slag was produced at a steelworks (JFE Steel Corp.) as a by-product and had a diameter of 1 to 3 cm. The chemical composition of the steel-slag was analyzed using an X-ray-fluorescence (XRF) spectrometer (XRF-1800, SHIMADZU) and the results are shown in Table 1.

Installation and operation of the in situ experiment

A schematic of the experimental setup is shown in Fig. 2. Four polyethylene containers with a height of 30 cm and a diameter of 30 cm were buried 15 cm deep in the seabed by diver. One container was left as is during the experiment to provide a control while steel-slag and/or an SMFC were configured in the other three containers. These are referred to as Steel-slag, SMFC, and SS-SMFC, respectively. Note that only the electricity production of the SMFC and SS-SMFC are discussed in this paper while the organic matter and the benthic environment will be discussed in a subsequent paper. Both the steel-slag and the anode electrode were placed at a height of 15 cm above the bottom of the container and the cathode was attached to a buoy located on the surface of the sea. The environmental conditions, such as the water depth, water temperature, and concentration of dissolved oxygen (DO), are listed in Table 2.

While no sediments were included in the containers when the experiment began, the setup was such that sediments were allowed to settle naturally into the containers to confirm the sustainability of the SMFC system in a sedimentary environment. The experiment was conducted from January 30, 2017 to December 11, 2018 and the actual water temperature and DO changes were measured during the initial stages of the experiment (January 2017 to August 2017).

A polarization curve, which is used to display the voltage output of a fuel cell for a given current density loading and is one of the most common methods of evaluating a fuel cell, was obtained via a test conducted using linear sweep voltammetry on the 589th day after installation using an external resistor housed in a data box whose resistance was varied from 1.9 to 11,500 Ω. The voltage for each resistance value was recorded after allowing a sufficient amount of time for the current to stabilize (5 min).

Results

Maintenance of the SMFC system

As shown in Figs. 4 and 5, the two-year experiment was divided into four periods during which the temporal changes in the anode potential and current density were assessed. Maintenance tasks were performed on the system whenever the electric power output was observed to degrade, presumably due to equipment problems.

The periods were defined as follows. At the beginning of the experiment, which was coincident with the start of Period 1, the cathode was assembled by attaching carbon fiber to a round plastic rod to ensure a large surface area (Fig. 3(a)). Then, on the 162th day, which was defined as the start of Period 2, the cathode appeared to become semi-permanently damaged as a result of the current density (Fig. 4). At the beginning of Period 3 (505th day, June 19, 2018), the cathode was replaced by one with an improved morphology in which plastic netting was applied to reduce interference from impurities (Fig. 3(c)). While this new cathode was divided into two parts, the amount of carbon fiber used was the same as that in the previous one. Period 4 began after 575 days when the SMFC circuit remained open for about 28 days and had to be repaired. To prevent future disconnections, the SMFC and SS-SMFC circuits were connected directly to share the two cathodes as a terminal for electron transport from each anode.

Anode potential

The temporal changes in the anode potential are shown in Fig. 4. In Period 1, the SMFC system was left open circuit for nine days to determine the lower limit of the anode potential and was found to be 13 and -620 mV for the SMFC and SS-SMFC cases, respectively. Electron-harvesting by the SMFC began on the tenth day. In Period 1, the anode potential was 88.9 ± 4.7 and -191.7 ± 61.2 mV for the SMFC and SS-SMFC cases, respectively, from days 10 to 40, and as the anode potential increased, there was no significant difference observed in the anode potential of these two cases between days 40 to 160. In Period 2, the anode potential was 481.9 ± 201.1 and -159.5 ± 137.2 mV for the SMFC and SS-SMFC, respectively, from days 180 to 505. In Period 3, the anode potential was 134.7 ± 93.9 and -217.1 ± 98.1 mV for the SMFC and SS-SMFC cases, respectively, from days 510 to 540. There was no significant difference in the anode potential of the two cases in Period 4.

Current density

The temporal changes in the current density are shown in Fig. 5. In Period 1, the current density was 2.8 ± 3.2 and 64.8 ± 8.4 mA/m^2, respectively, for the SMFC and SS-SMFC cases during the first 60 days. It then gradually increased to 55.6 and

198.4 mA/m^2, respectively, at 160 days. In Period 2, the current density was 15.6 ± 10.9 and 54.8 ± 15.5 mA/m^2 for the SMFC and SS-SMFC cases, respectively, from days 180 to 505. In Period 3, the current density was 21.2 ± 5.4 and 150.4 ± 69.7 mA/m^2 for the SMFC and SS-SMFC cases, respectively, from days 510 to 570. Note that the SMFC case was in open circuit from days 545 to 580. In Period 4, current density increased to 16.8 ± 10.4 and 236.8 ± 87.7 mA/m^2 for the SMFC and SS-SMFC cases, respectively, from 580 to 680 days.

Polarization curve test

A polarization curve and the power density vs. the current density are shown in Fig. 6 where it can be seen that the maximum power density was 12.3 and 110.1 mW/m^2 for the SMFC and SS-SMFC cases, respectively, at current densities of 37.2 and 324.7 mA/m^2. An overvoltage based on the increase in the current was calculated as the difference between the maximum and minimum values of the voltage. The decrease in the gradient of the voltage vs. the current was -35.5 and -5.2 V/A for the SMFC and SS-SMFC cases, respectively. The maximum overvoltage was computed to be 0.60 and 0.48 V for the SMFC and SS-SMFC cases, respectively.

Discussion

Power generation

During the two years of SMFC operation, the total recovered charge (in coulombs) was determined by integrating the current produced over the period of operation and was found to be 168 and 1,053 kC for the SMFC and SS-SMFC cases, respectively (247 and 1,549 C/day). Note that Hong et al.[16] obtained a 7.9 C/day of charge from eutrophic stream sediments and Touch et al.[14] obtained 11.5 C/day of charge from riverbank sludge originating from sewage. A comparison of the power and current densities for the operating conditions between previous studies and this study are shown in Table 3, where it can be seen that the performance of the fuel cells in this study were superior to the others in terms of the power density, and the amount of current generated was remarkably high. As the focus of the current study was on the biodegradation of contaminated sediment rather than power generation, the external resistance was relatively low in comparison to maximize current generation. Although it is difficult to compare the results of one study to those of others in the literature because of differences in the operating conditions (e.g., the electrode material, external resistance, etc.) of the SMFC,[14] the addition of steel-slag enabled the highest power generation at a considerably lower external resistance. Thus, it is anticipated that steel-slag will prove to be a viable means to overcome the limitations of conventional SMFC technology.

Roles of steel-slag on SMFC performance

One of the primary benefits of employing steel-slag is to increase power production by lowering the anode potential beyond the equilibrium of the redox potential of SO_4^{2-} / H_2S. The electron acceptor having the lowest potential in seawater is sulphate, and the redox potential of contaminated marine sediments drops to -420 mV (vs. Ag / AgCl) of the SO_4^{2-} / H_2S equilibrium potential. Thus, current production in conventional SMFCs depends on the presence of sulfur species around the anode electrode; however, the addition of steel-slag removes this restriction. It was confirmed that steel-slag decreased the anode potential to -620 mV during open circuit until the ninth day due to the equilibrium redox potential of Fe / Fe^{2+} at -646 mV.

Sediment began to flow into the containers after the 75th day, after which the current density increased continuously until the 150th day (Fig. 5). The correlation between the anode potential and current density in this period is shown in Fig. 7. The steel-slag increased the gradient of the current density vs. the anode potential more than ten times that of the SMFC alone and this increase was accompanied by a significant increase in the efficiency of current production. In the case of the SMFC, the anode potential increased to a maximum of 400 mV, which suggests that the anode was affected by DO in the water layer. As the reduction of the oxygen content is an important factor in an SMFC, the effects of oxygen on current production are discussed in detail below. The presence of steel-slag suppressed the maximum increase in the anode potential to around 200 mV by the oxidation reaction of Fe despite the interruption of the oxygen. The major effect of the steel-slag was to increase the amount of current by lowering the anode potential as described above. Nevertheless, the increase in the current density gradient was not related to the anode potential. For the same anode potential (at 100 mV for instance), steel-slag increased the current density about 7.4 times compared to that of the SMFC (31.7 and 234.1 mA/m^2 for the SMFC and SS-SMFC, respectively). Thus, the increase in the current density gradient can also be attributed to the steel-slag. Organic matter is known to be redox reactive with Fe(III)-containing minerals.[21] For example, Lovley[22] investigated the oxidation mechanism of soil humic acid which is non-biodegradable organic matter and found it to be a consequence of the reduction of Fe(III). Based on these findings, the carboxyl (e.g., acetate) and phenolate groups that are the most abundant functional groups in humic acid can be oxidized with Fe(III) minerals as follows:

$$\text{acetate}^- + 8\text{Fe}^{3+} + 4\text{H}_2\text{O} \rightarrow 2\text{HCO}_3^- + 2\text{Fe}^{2+} + 9\text{H}^+, \quad (1)$$

$$\text{phenol} + 28\text{Fe}^{3+} + 17\text{H}_2\text{O} \rightarrow 6\text{HCO}_3^- + 28\text{Fe}^{2+} + 34\text{H}^+. \quad (2)$$

In these equations, solid-phase Fe(III) minerals accept electrons from organic matter, and are then reduced to release soluble Fe^{2+}. Therefore, the Fe oxide contained in the steel-slag stimulates the dissolution of non-biodegradable organic matter, which can then be used as fuel for the SMFC. It is believed that these characteristics of steel-slag contributed toward increasing the gradient of the current density per anode potential. However, most common organic materials do not nonenzymatically react with Fe(III). Although the electron-harvesting capability of SMFCs has been expected to act as a catalyst for the interaction of steel-slag and humic acid, the exact mechanism has not yet been elucidated.

The results of a polarization curve test show that the addition of steel-slag increased the maximum power density by nine times compared to that of the SMFC alone (Fig. 6). In addition, overvoltages were decreased by 0.12 V by the steel-slag. These results validate the hypothesis regarding the role of the Fe in steel-slag in that steel-slag not only provides electrons, but also stimulates electron transmission. In a current–voltage diagram of two fuel cells, it is possible to distinguish three different types of losses, namely, activation, ohmic, and concentration losses.[14] Concentration losses occur when the available electron donors (ED) are transported away from the electrode after being consumed. Thus, the concentration loss during times of limited mass transport became increasingly noticeable at higher levels of current density. In contrast, the addition of steel-slag enabled high levels of power generation with little concentration loss because the Fe in the steel-slag made up for the drop in EDs during transport.

Influence of external factors on SMFC performance

The current density results indicated that the current generation was limited in the early part of Period 1 (up to 75 days) and Period 2 (Fig. 5). In the case of Period 2, this was thought to be due to short-term heavy rainfall that accompanied sewage discharge as the resulting hydraulic vortices likely removed sediments from the experimental containers. The relatively high anode potential during this period should be attributed to the reduction of oxygen at the surface of the anode when it was not completely immersed in sediment (Fig. 4). While oxygen is generally consumed as an electron acceptor in cathodic reactions, the presence of dissolved oxygen near the anode directly consumed electrons and increased the anode potential to the O_2 / H_2O equilibrium potential (600 mV at pH 7). The DO present near the anode eventually hindered the electron-harvesting of the SMFC. Wang et al.[23] constructed wetland-MFC systems to investigate organic and nutrient removal and reported results that were similar to ours in that the presence of excessive DO has the potential to significantly disturb the anaerobic environment in the anode zone, which will be detrimental to power generation and organics degradation operations. Hong et al.[10] suggested that the critical DO concentration for current generation in an SMFC is 3 mg/L. In other words, current generation is not notably affected by the DO concentration until it falls below 3 mg/L at the cathode. It should be noted that oxygen depletion occurs frequently in the summer at the location where this study was conducted, and the mean DO concentration in summer was 0.35 mg/L and that in winter was 10.49 mg/L (Table 2). Thus, since DO concentrations can vary dramatically in marine environments, DO is thought to be a further limiting factor during the practical operation of an SMFC.

The gradient of the current density per anode potential in Periods 3 and 4 are shown in Fig. 8 (SS-SMFC only). Compared to the results in Period 1, which are shown in Fig. 7, the minimum value of the anode potential decreased from -110 to -450 mV in Period 3 (from 510 to 540 days). The reduction in anode potential is evidence that the anode was fully buried within the sediment, and the corresponding gradient of the current density increased from 0.53 to 0.65. Kubota et al.[24] investigated changes in the power production vs. the depth to which the anode was embedded and concluded that the anode depth had a significant effect on the power generation of the SMFC. They determined that an SMFC using an anode placed at the surface of the sediment exhibited a very low power density of 3.0 mA/m^2 compared with an anode placed deep in the sediment (16.5 mA/m^2). This result is consistent with our findings and suggests that it is essential to maintain the anode in a reduced state to ensure the continuous production of current.

Early in Period 4 (from 600 to 630 days), the maximum current production increased by 1.5 times compared to that in Period 3 without a gradient change (Fig. 8). The absence of a gradient change indicates the performance of the cathode increased without changing the anode conditions. That is, the increase in current production appears to be related to maintenance performed coincident with the start of Period 4 (see Section 3.1). Since amount of current density in the SMFC was significantly smaller than that of the SS-SMFC (16.8 and 236.8 mA/m^2, respectively), connecting two circuits between the SMFC and SS-SMFC doubled the cathode area of the SS-SMFC. In the case of an MFC, it is generally recommended that the cathode area should be larger than that of the anode. In contrast, an SMFC may not require such a large cathode area as the rate of the anodic reaction (i.e., the oxidation of substances in the sediment) is considerably lower than that observed in an MFC provided with a continuous feed of labile organic matters, such as acetate and glucose.[10] Dentel et al.[25] reported that current production is not limited by a cathode with a five times smaller surface area than that of an anode when generating electricity from wastewater sludge. In addition, in our pre-investigation conducted in the Fukuyama inner bay, we investigated the current when the cathode area of the SMFC was increased up to 18 times compared to the anode but found no significant differences. In this study, the supply of electrons from the steel-slag surpassed our expectations and the increase in the current density depending on the cathode area confirms that a significant amount of oxidation reaction occurred due to the steel-slag.

The daily change in the anode potential from the beginning of Period 3 is shown in Fig. 9, where it can be seen that the daily change in potential was irregular after the cathode was replaced with the new morphology at the 505th day. However, from 514th day onward, the anode potential appeared to be affected by the tide. This tendency suggests that a flood tide with sufficient DO may affect the performance of the cathode. The anode potential reached its maximum at around midday, and this pattern remained consistent throughout Periods 3 and 4. The current density exhibited the same daily cycle of the potential (Fig. 10(a)). In Periods 3 and 4, the mean current density in the day increased by 59 and 68%, respectively, compared to that in the night and a current density of at least 100 mA/m^2 always occurred during the daytime, but fell to zero at night. This was attributed to the activity of microorganisms, such as the photosynthesis of algae attached to the cathode.

Biofilm growth on the cathode in field experiments is inevitable as the cathode is usually exposed in an aqueous environment with a diverse microbial community. This microbial activity is expected to obviate the need for an external oxygen supply. The cathode potential exhibited the same daily cycle as the current density. In Periods 3 and 4, the average cathode potential during the day increased by 64 and 262%, respectively, compared to that at night (Fig. 10(b)). Nonetheless, the maximum value of the cathode potential was the same in both the day and night. Previous researchers[26,27] mentioned that microbially-catalyzed redox reactions may affect the maximum cathode potential and reported that the development of biofilm on the cathode increased the cathode potential to 286 and 384 mV vs. Ag/AgCl, respectively, in an SMFC with a carbon-based cathode. Therefore, algal activity may have influenced the maximum cathode potential of each period, although the cathode potentials may differ depending on the conditions of the SMFC system and microbial species. For reference, it was reported that some aerobic microbes, such as *Pseudomonas* and *Novosphigobium*, may exist predominantly at the cathode in an oxic environment.[28] Although information on the microbial diversity and their biocatalytic functions is still very limited, our findings suggest that algal activity in the field appeared quickly (within nine days), which led to the control of the maximum cathode potential and a considerable increase in the current density during the day.

Conclusions

The benefit of adding steel-slag and the influence of external factors were investigated during in situ operation of an SMFC over a two year period. The presence of steel-slag was found to increase the current density by decreasing the anode to Fe oxidation potential. The oxidation of Fe provided substitutes for electron donors during transport, which decreased the concentration loss in the anode. It is thought that that steel-slag likely stimulates current acquisition for the same anode potential by encouraging the dissolution of non-biodegradable organic matter by the iron oxide in the steel-slag. During in situ operation, it was essential to maintain the anode in a reduced state to ensure the continuous production of current. If hydraulic vortices due to rainfall carry away sediments, it can allow the anode to become exposed to an oxic water layer. The cathode was found to be more sensitive to changes in the external environment, and the attachment of a non-conductor caused semi-permanent damage to the cathode. In contrast, algal activity in real field appeared within nine days, which led to a control of maximum cathode potential and considerable increase of current density during daytime. It is anticipated that the results of this study will prove valuable for operators of in situ SMFCs that use steel-slag in the development of practical SMFCs.

Conflicts of interest

There are no conflicts to declare.

Acknowledgements

The acknowledgements come at the end of an article after the conclusions and before the notes and references. Note that all sources of funding should be declared.

Notes and references

1 N. Touch, T. Hibino, N. Kinjo, and Y. Morimoto, *Int. J. Environ. Sci. Technol.*, 2018, **15**, 507–512.
2 K. Jessoe, *J. Environ. Econ. Manage.*, 2013, **66,** 460–475.
3 W.-W. Li and H.-Q. Yu, *Biotechnol. Adv.*, 2015, **33**, 1–12.
4 N. Song, H.-L. Jiang, H.-Y. Cai, Z.-S. Yan, and Y.-L. Zhou, *Chem. Eng. J.*, 2015, **279**, 433–441.
5 Y.-L. Zhou, H.-L. Jiang, and H.-Y. Cai, *J. Hazar. Mater.*, 2015, **287**, 7–15.
6 W.-W. Li, H.-Q. Yu, and Z. He, *Energy Environ. Sci.*, 2014, **7**, 911–924.
7 S.T. Oh, J.R. Kim, G.C. Premier, T.H. Lee, C. Kim, and W.T. Sloan, *Biotechnol. Adv.*, 2010, **28**, 871–881.
8 H. Wang and Z.J. Ren, Z.J. *Biotechnol. Adv.*, 2013, **31**, 1796–1807.
9 Z. Yan, N. Song, H. Cai, J.-H. Tay, and H. Jiang, *J. Hazar. Mater.*, 2012, **199–200**, 217–225.
10 S.W. Hong, I.S. Chang, Y.S. Choi, T.H. Chung, *Bioresour. Technol.*, 2009, **100**, 3029–3035.
11 D.A. Lowy, L.M. Tender, J.G. Zeikus, D.H. Park, and D.R. Lovely, *Biosensors and Bioelectron.*, 2006, **21**, 2058–2063.
12 F. Zhao, F. Harnisch, U. Schröder, F. Scholz, P. Bogdanoff, and I. Herrmann, *Environ. Sci. Technol.*, 2006, **40**, 5193–5199.
13 K. Kim, K. Nishimura, K. Yoshimura, and T. Hibino, *J. Jpn. Soc. Civ. Eng. B2 (Coastal Eng.)* (in press), 2019.
14 N. Touch, T. Hibino, Y. Nagatsu, and K. Tachiuchi, *Bioresour. Technol.*, 2014, **158**, 225–230.
15 Y. Nagatsu, K. Tachiuchi, N. Touch, and T. Hibino, *J. Jpn Soc. Civ. Eng. B2 (Coastal Eng.),* 2014, **70**, 1066–1070 (in Japanese with English abstract).
16 S.W. Hong, H.S. Kim, and T.H. Chung, *Environ. Pollut.*, 2010, **158**, 185–191.
17 J.M. Morris and S. Jin, *J. Hazar. Mater.*, 2012, **213–214**, 474–477.
18 T.S. Song and H.L. Jiang. *Bioresour. Technol.*, 2011, **102**, 10465–10470.
19 N. Song and H.L. Jiang. *Int. J. Hydrogen Energy*, 2018, **43**, 10082–10093.
20 L.M. Tender, C.E. Reimers, H.A. Stecher, D.E. Holmes, D.R. Bond, D.A. Lowy, K. Pilobello, S.J. Fertig, and D.R. Lovely, *Nat. Biotechnol.*, 2002, **20**, 821–825.
21 J. Chen, B. Gu, R.A. Royer, and W.D. Burgos, *Sci. Total Environ.*, 2003, **307**, 167–178.
22 D.R. Lovley, *Microbiol. Rev.*, 1991, **55**, 259–287.
23 X. Wang, Y. Tian, H. Liu, X. Zhao, and S. Peng, *Sci. Total Environ.*, 2019, **653**, 860–871.
24 K. Kubota, K. Kusunoki, T. Watanabe, H. Maki, and K. Syutsubo, *J. Jpn. Soc. Water Environ.*, 2017, **40**, 51–57. (in Japanese with English abstract)
25 S.K. Dentel, B. Strogen, and P. Chiu, *Water Sci. Technol.*, 2004, **50**, 161–168.
26 L.D. Schamphelaire, L.V.D. Bossche, H.S. Dang, H. Höfte, N. Boon, K. Rabaey, and W. Verstraete, *Environ. Sci. Technol.*, 2008, **42**, 3053–3058.
27 C.E. Reimers, P. Girguis, H.A. Stecher III, L.M. Tender, N. Ryckelynck, and P. Whaling, *Geobiol.*, 2006, **4**, 23–136.
28 B. Erable, I. Vandecandelaere, M. Faimali, M.-L. Delia, L. Etcheverry, P. Vandamme, and A. Bergel, *Bioelectrochem.*, 2010, **78**, 51–56.

Table 1. Chemical elements in the steel-slag.

Element (%)			
CaO	36.7	SiO_2	23.1
Fe_2O_3	17.9	MgO	4.1
MnO	3.7	Al_2O_3	3.4
P	1.7	TiO_2	1.2

Table 2. Environmental conditions of the experiment area in winter and summer of 2017 (Jan. 30 to Feb. 28 and Jul. 9 to Aug. 9, respectively).

		Depth (m)	Temp. (℃)	Salinity (psu)	DO (mg/L)	EC (mS/cm)
Feb.-2017	Max.	5.2	11.3	31.8	15.95	35.4
	Min.	1.3	8.4	30.8	5.14	33.2
	Ave.	3.4	10.0	31.5	10.49	34.7
Jul.-2017	Max.	5.5	29.0	30.6	2.59	49.0
	Min.	1.5	21.9	27.3	0.07	14.2
	Ave.	3.6	24.7	29.5	0.35	45.3

Table 3 Comparison of the maximum output and operating conditions of the SMFC.

Power density (mW/m^2)	Current density (mA/m^2)	Operating conditions	Reference
2	17	Eutrophic stream / Graphite felt / 10 Ω	10
6	14	Polluted beach / Carbon cloth / 1000 Ω	17
8	250	Tidal river / Carbon cloth / 100 Ω	14
13	6	Eutrophic lake / Graphite felt / 1000 Ω	18
25	–	Lake / Graphite felt / 1000 Ω	19
31	75	Salt marsh / Graphite disk / -	20
2	79	Brackish river / Carbon cloth / 1.4 Ω	This study (SMFC)
57	476	Brackish river / Carbon cloth / 1.4 Ω	This study (SS-SMFC)

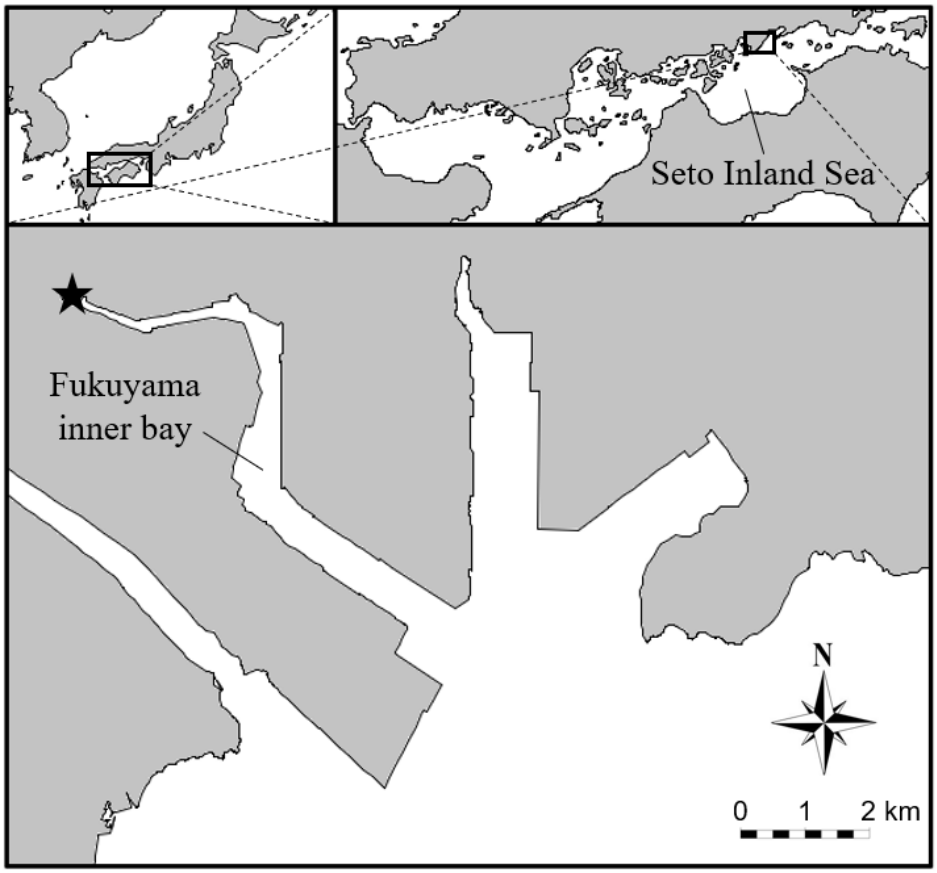

Fig. 1. Topographical map of the Fukuyama Inner Bay (the area of the experiment is denoted by the asterisk).

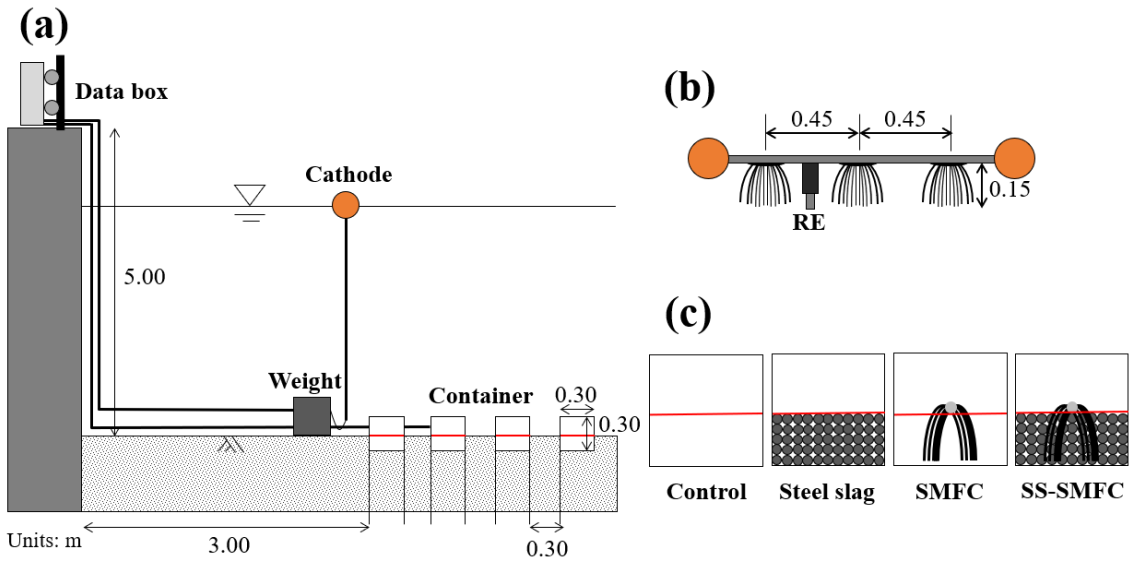

Fig. 2. Schematic diagram for experimental setup (a) and the detailed conditions of the cathode (b) and anode (c) areas. Each container at the anode area refers to the experimental cases. Containers were buried with the red line parallel to the sediment surface. The voltage recorder and external resistance were secured in a data box. RE refers to the reference electrode (vs. Ag/AgCl).

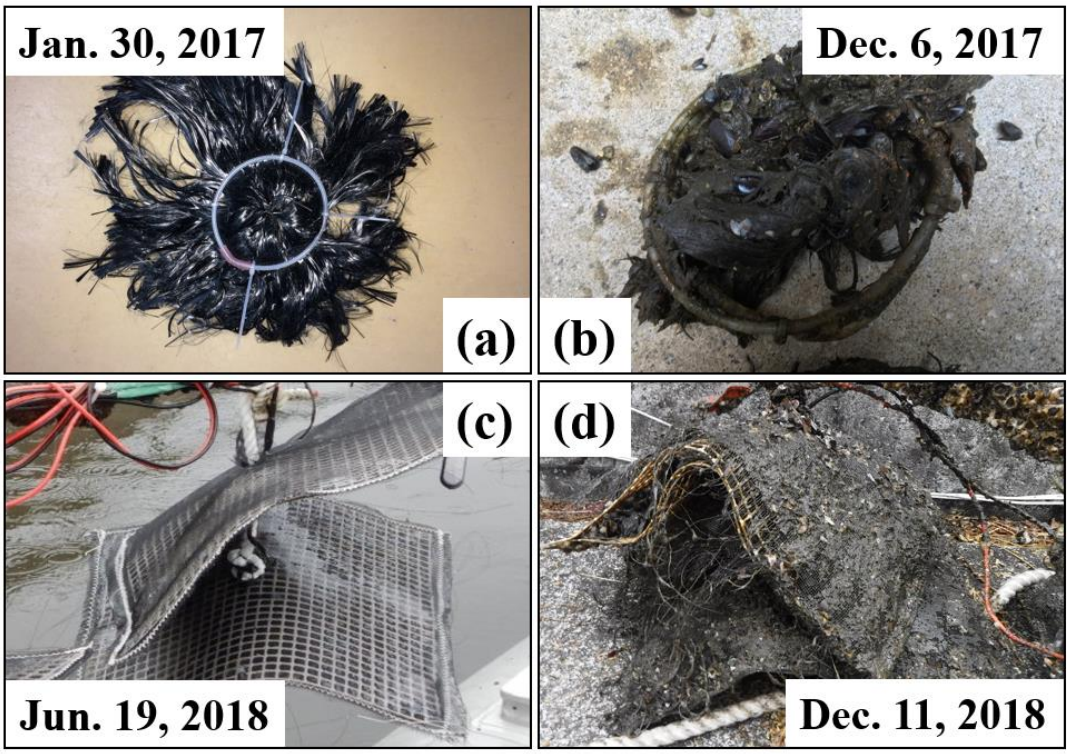

Fig. 3. Before (a, c) and after (b, d) use of two types of cathode electrode.

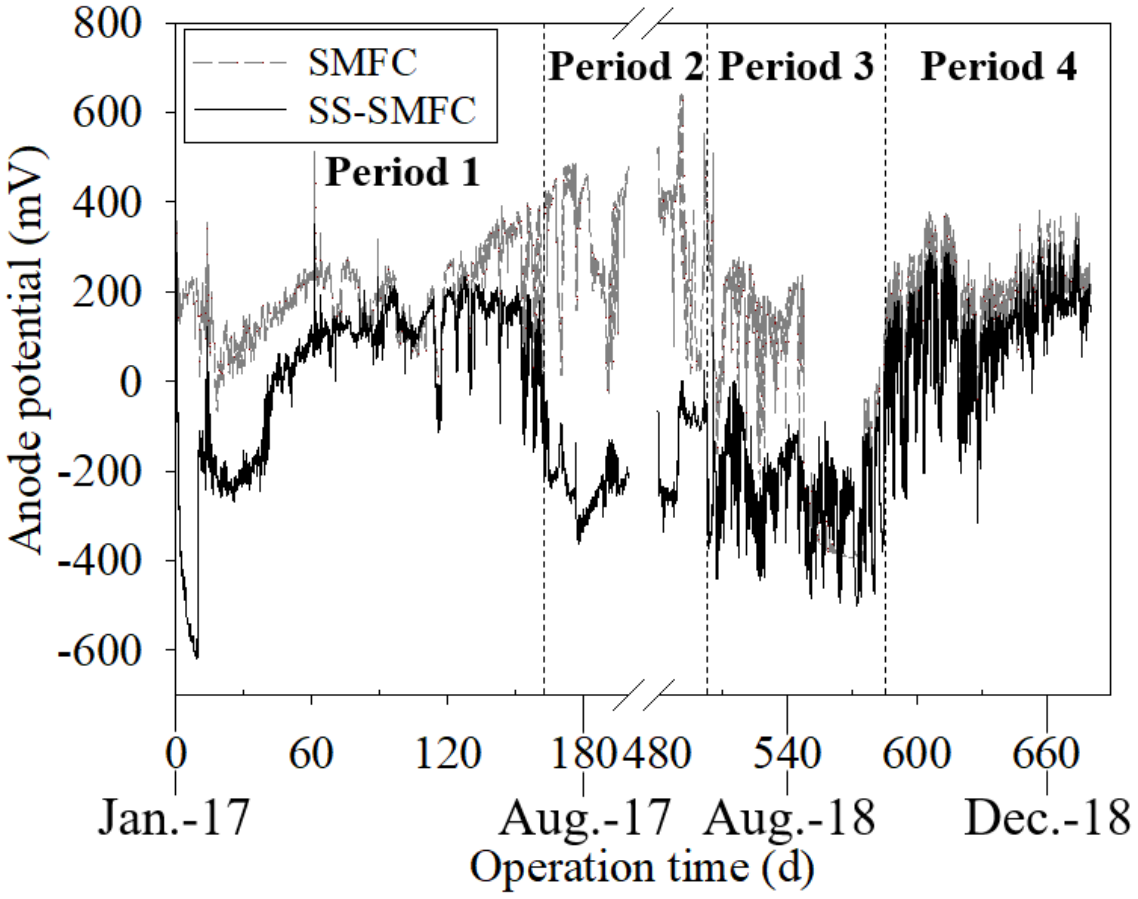

Fig. 4. Temporal variation of the anode potential (mV vs. Ag/AgCl) in the SMFC system. Note the period between 200 and 480 days was omitted.

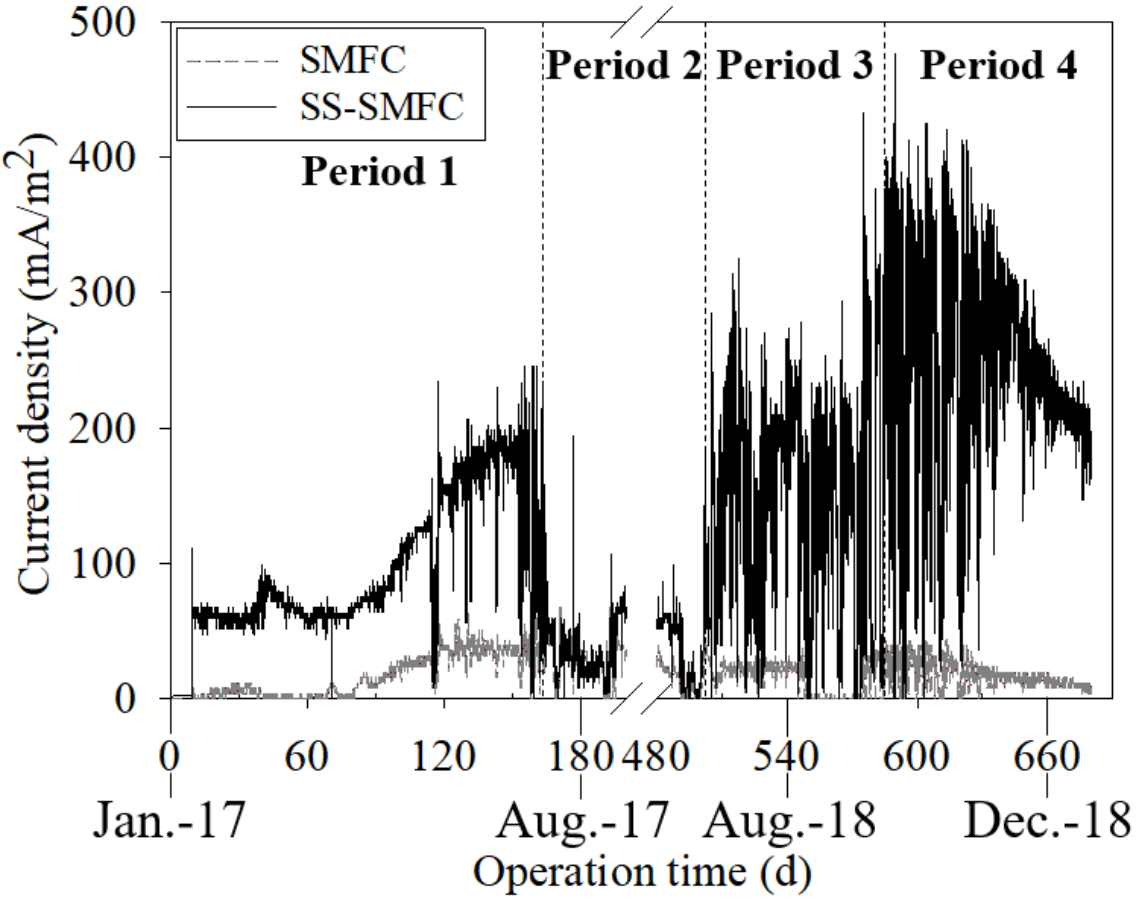

Fig. 5. Behavior of the current density in an SMFC system. Note the period between 200 and 480 days was omitted.

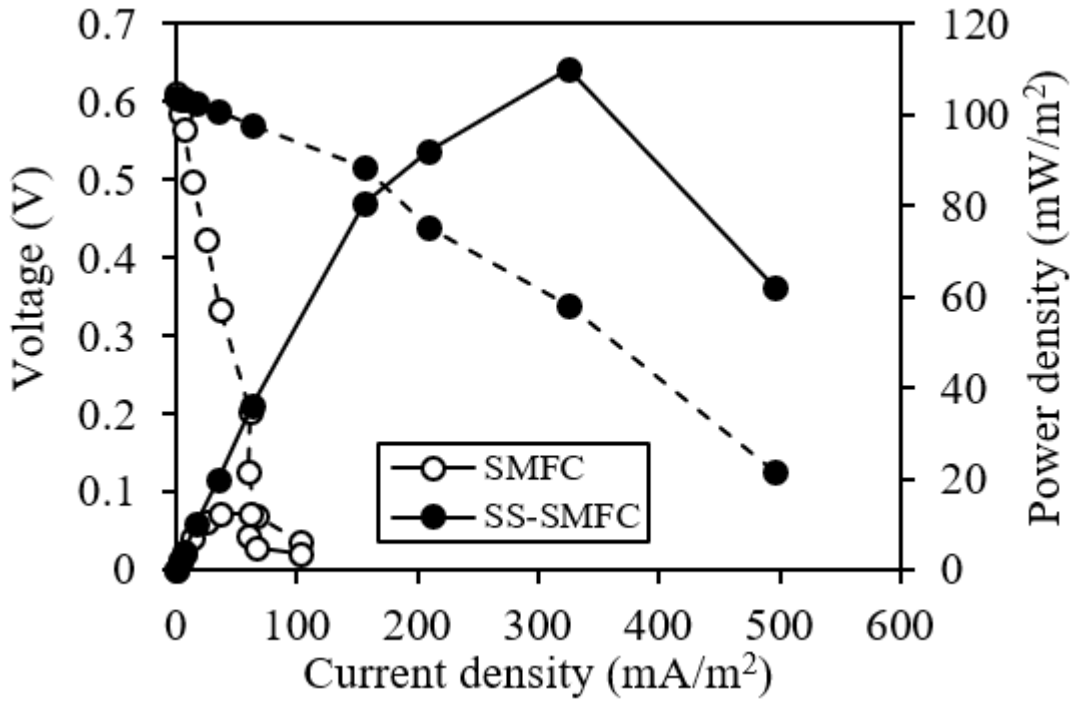

Fig. 6. Voltage (dotted line) and power density (solid line) as a function of the current density obtained on the 589th day after installation.

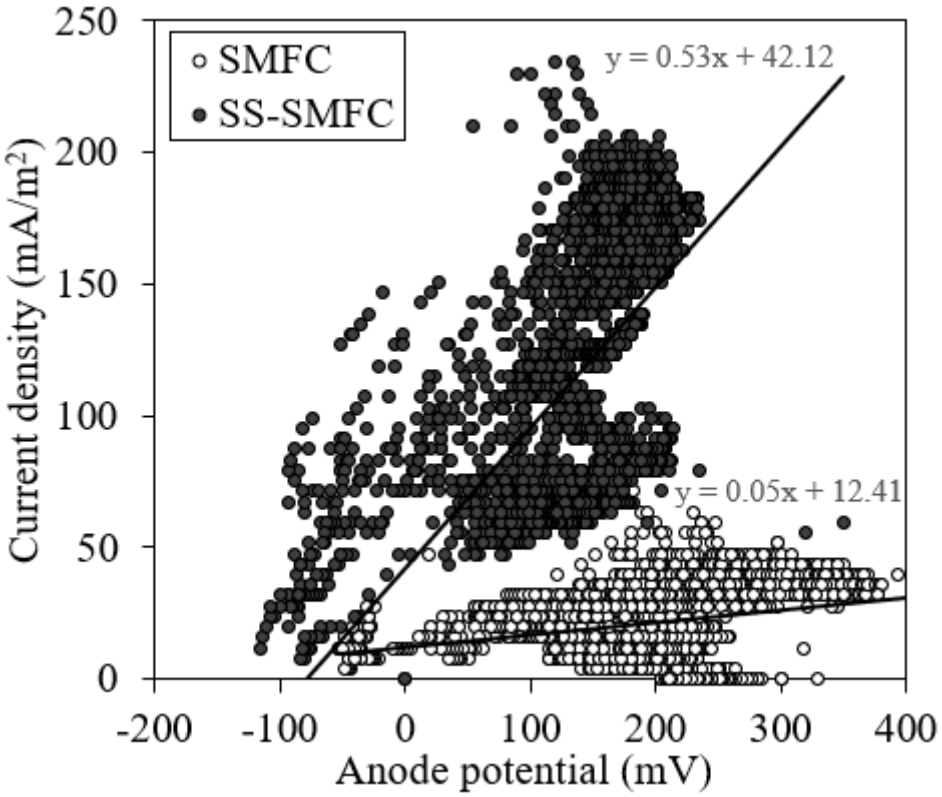

Fig. 7. Correlation between the current density and anode potential from days 75 to 150.

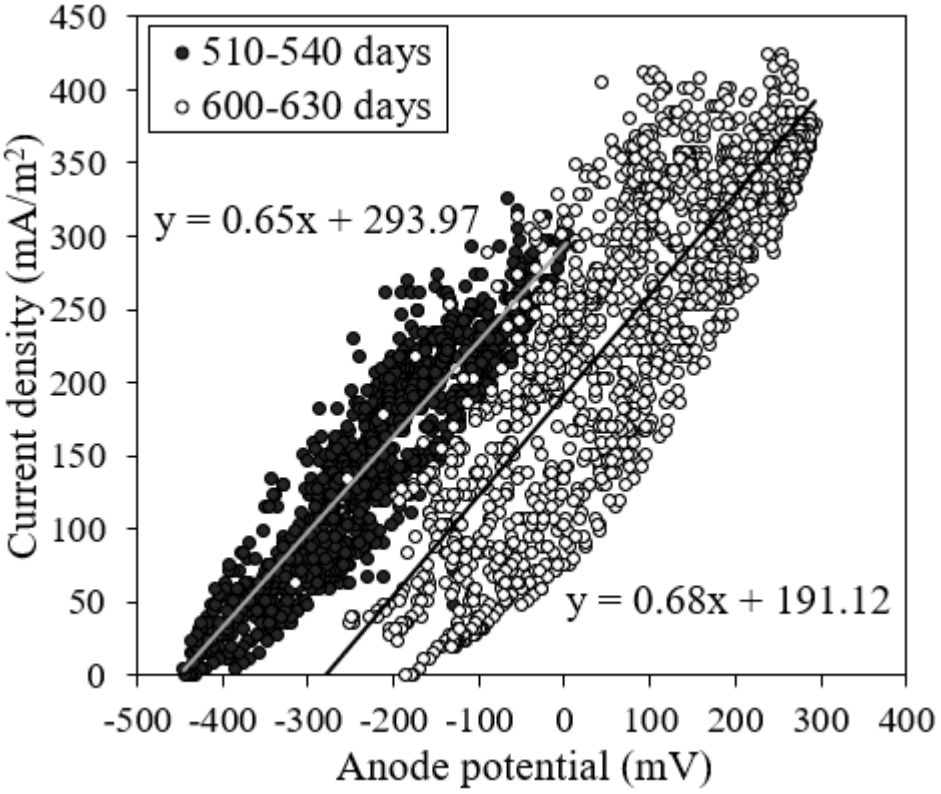

Fig. 8. Correlation between the current density and anode potential in the SS-SMFC during Periods 3 and 4.

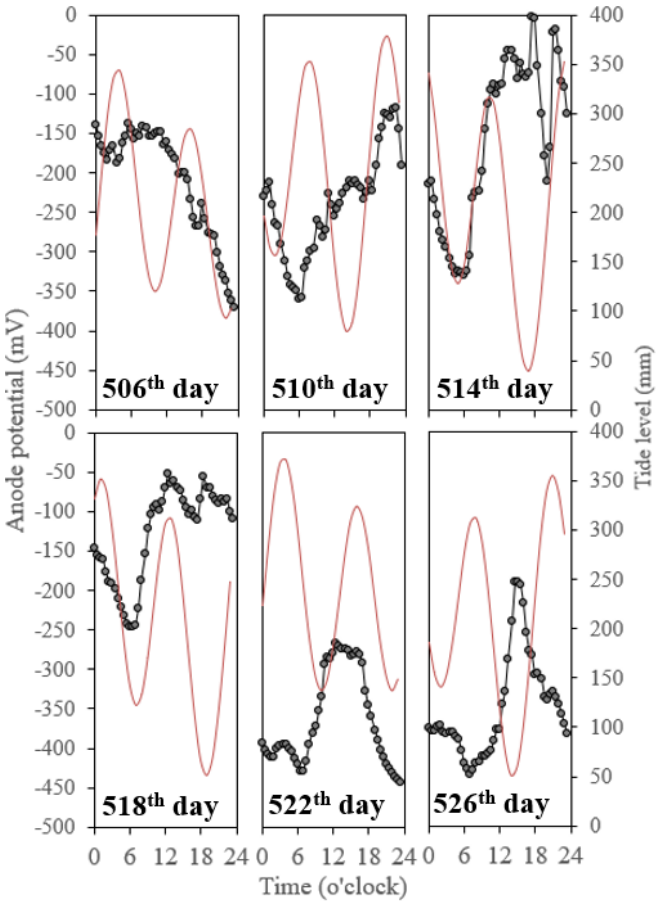

Fig. 9. Daily change in the anode potential of the SS-SMFC (the line with symbols) and tide (the red solid line) from replacement of the cathode on the 505th day.

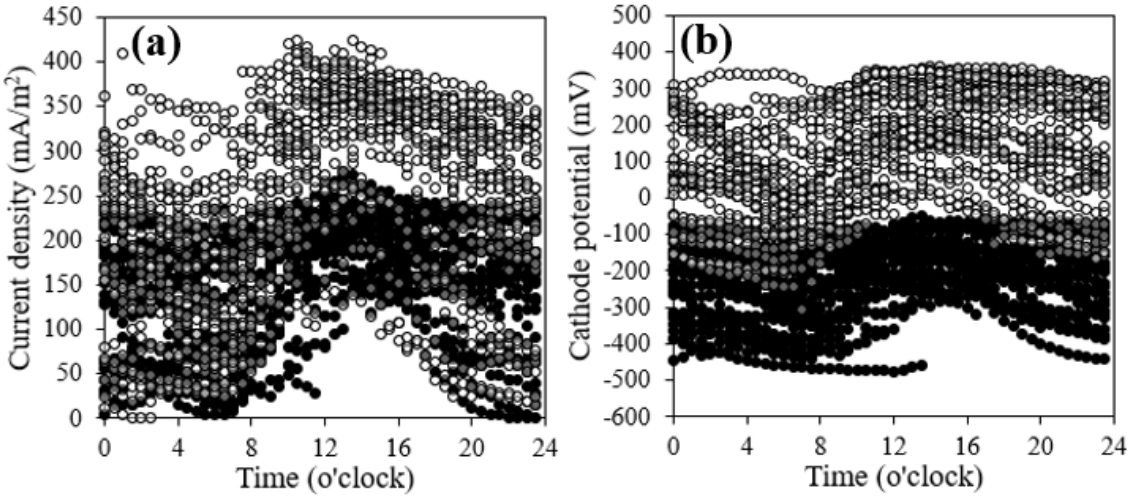

Fig. 10. Daily change in (a) the current density and (b) cathode potential of the SS-SMFC. The black and white symbols indicate Period 3 (520 to 550 days) and Period 4 (600 to 630 days), respectively.